On the Existence of the Double Scroll Attractor for the Chua's Circuit with a Smooth Nonlinearity

Zbigniew Galias
AGH University of Science and Technology
Department of Electrical Engineering
al. Mickiewicza 30, 30–059 Kraków, Poland
Email: galias@agh.edu.pl

Warwick Tucker
Uppsala University
Department of Mathematics
Box 480, 751 06 Uppsala, Sweden
Email: warwick@math.uu.se

***Abstract*—In simulations of the Chua's circuit with a smooth nonlinearity for certain parameter values one observes the double scroll attractor. This attractor contains an unstable equilibrium, and typical trajectories belonging to the attractor may pass arbitrarily close to this equilibrium. In consequence, it is impossible to compute trajectories over the whole attractor using standard rigorous numerical integration procedures. This is due to the existence of trajectories which spend arbitrarily long time in a neighborhood of the equilibrium. In this work, a method to find enclosures of trajectories passing arbitrarily close to an unstable fixed point of spiral type is presented. This method is used to prove the existence of a trapping region enclosing the double scroll attractor for the Chua's circuit with a cubic nonlinearity.**

I. Introduction

The Chua's circuit [1] is perhaps the most famous example of an electronic circuit displaying chaotic dynamics. The existence of various dynamical phenomena in this system has been studied extensively in the literature [2], [3], [4], [5], [6], [7], [8], [9], [10].

Most of the results presented in the literature are based on simulations of the circuit and analysis of geometrical models of corresponding attractors. The first rigorous result concerning the existence of chaos in the Chua's circuit was given in [3], where the existence of a Shilnikov-type homoclinic orbit is proved. A computer-assisted proof of chaotic behavior (more precisely of positive topological entropy) for the double scroll attractor was presented in [7]. In [11], it was shown that there exist a trapping region for the double scroll attractor. A rigorous study of the spiral attractor was carried out in [12]. The results listed above concern the circuit with a piece-wise linear characteristic of the Chua's diode.

Dynamical phenomena of the Chua's circuit with a cubic nonlinearity were first analyzed in [13]. Various types of bifurcations were studied via numerical simulations. An electronic implementation of the cubic nonlinearity using two multipliers and one operational amplifier was presented in [14]. In [15], for the case of a spiral attractor the existence of a trapping region has been proved using rigorous integration methods. It was explained why available rigorous integration tools cannot be applied to prove the existence of a trapping region for the case of the double scroll attractor, which contains an unstable equilibrium. The Chua's circuit with a different type of a smooth nonlinearity was considered in [16]. In this paper, we continue the analysis of the double scroll attractor for the Chua's circuit with a cubic nonlinearity. We present a rigorous method for the computation of trajectories in a neighborhood of an unstable equilibrium. Using this method, we prove the existence of a trapping region for the double scroll attractor.

The layout of the paper is as follows. In Section II the definition of the circuit is recalled and its properties are discussed. In Section III we describe a method how to compute enclosures of trajectories passing close to an unstable equilibrium and prove that a certain set is a trapping region for the double scroll attractor.

II. The Chua's Circuit with a Cubic Nonlinearity

The Chua's circuit [13] shown in Fig. 1 is composed of two capacitors C_1, C_2, one inductor L, two linear resistors R_0, R and one nonlinear resistor R_N. The i-v characteristics of the nonlinear resistor is a polynomial of order three $i = g(v) = g_1 v + g_2 v^3$. Let us denote by x_1 and x_2 the voltages over the capacitors C_1 and C_2 and by x_3 the current flowing through the inductor L. The dynamics of the circuit is defined by the following differential equation

$$\begin{aligned} C_1\dot{x}_1 &= (x_2 - x_1)/R - g(x_1), \\ C_2\dot{x}_2 &= (x_1 - x_2)/R + x_3, \\ L\dot{x}_3 &= -x_2 - R_0 x_3. \end{aligned} \tag{1}$$

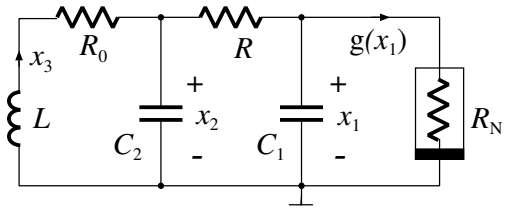

Fig. 1. The Chua's circuit.

Let us note that the system (1) is symmetric with respect to the transformation $(x_1, x_2, x_3) \mapsto (-x_1, -x_2, -x_3)$. It follows that if $x(t) = (x_1(t), x_2(t), x_3(t))$ is a trajectory of the system then also $-x(t)$ is a trajectory.

We consider the system (1) with the following set of dimensionless parameters: $C_1 = 0.7$, $C_2 = 7.8$, $L = 1.891$,

$R_0 = 0.01499$, $g_1 = -0.59$, $g_2 = 0.02$, and $R = 2.0$. For these parameter values the double scroll attractor is observed in simulations. An example trajectory is shown in Fig. 2.

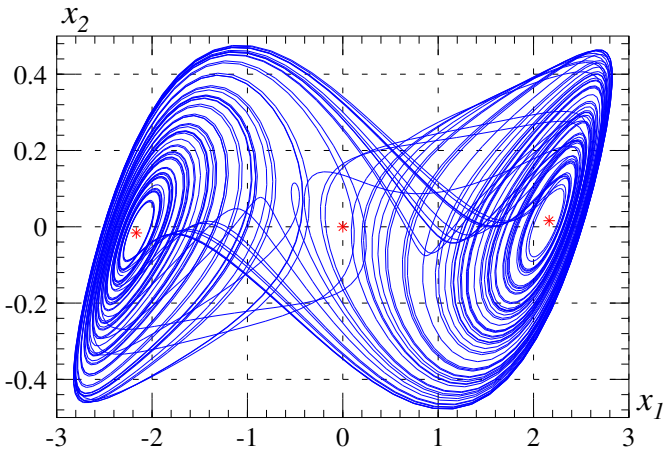

Fig. 2. An example trajectory of the circuit.

For the parameter values considered, the dynamical system (1) has three unstable equilibria, the origin $(0,0,0)$ and a symmetric pair of equilibria $\pm x^\star = (\pm x_1^\star, \pm x_2^\star, \pm x_3^\star) \approx \pm(2.164712700, 0.0161038235, -1.074304438)$, where $x_1^\star = \sqrt{-(g_1 + (R+R_0)^{-1})g_2^{-1}}$, $x_2^\star = R_0(R+R_0)^{-1}x_1^\star$, and $x_3^\star = -(R+R_0)^{-1}x_1^\star$. Positions of the equilibria are shown in Fig. 2 using the star symbol.

III. Analysis of the Double Scroll Attractor

In this section, we prove the existence of a trapping region enclosing the double scroll attractor. To reduce the continuous system (1) to a discrete one we use the method of the return map. Let $\Sigma = \Sigma_1 \cup \Sigma_2$ be the union of two planes $\Sigma_1 = \{x\colon x_1 = 2.1647\}$ and $\Sigma_2 = \{x\colon x_1 = -2.1647\}$. The *return map* $P : \Sigma \mapsto \Sigma$ is defined as $P(x) = \varphi(\tau(x), x)$, where $\varphi(t,x)$ is the trajectory of (1) based at x, and $\tau(x)$ is the return time after which the trajectory $\varphi(t,x)$ returns to Σ.

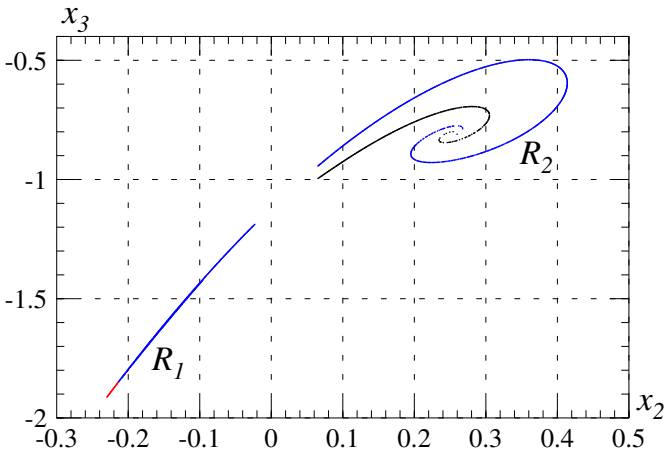

Fig. 3. Intersection of a trajectory of P with the plane Σ_1.

The intersection of an example trajectory of the return map P with the plane Σ_1 is shown in Fig. 3. The plot is composed of two parts R_1 and R_2. The set R_2 contains two spirals; the large one plotted in blue and the small one plotted in black. The intersection of trajectories of P with Σ_2 also contains two parts R_3, and R_4, which are symmetric to R_1 and R_2, respectively. Points belonging to R_2 are mapped by P to R_1. Blue points in R_1 are mapped to the larger spiral in R_2, while red points in R_1 are mapped to the smaller spiral in R_4.

In [15], the system (1) has been analyzed for the cases $R = 2.1$ and $R = 2.0$ for which in simulations one can see a spiral attractor and a double scroll attractor, respectively. For the case of the spiral attractor the existence of a trapping region has been proved. To show that a set $T \subset \Sigma$ is a trapping region we prove that $P(T) \subset T$. It is sufficient to prove that the image of the border ∂T of T is enclosed in T and that the return map is well defined on T (for details see [17]). The first part can be done by covering ∂T by boxes $\mathbf{v}_k$ (two-dimensional interval vectors), finding enclosures $\mathbf{y}_k$ of $P(\mathbf{v}_k)$, and verifying conditions $\mathbf{y}_k \subset T$. To prove that the return map P is well defined on T the whole set T is covered by boxes and enclosures of their images are found. The evaluation of P is done by rigorous integration of the vector field using the Lohner method [18]. The integration procedure was written in C++ using Profil/BIAS packages [19] for interval arithmetic computations. Part of the computations have been performed using the CAPD library [20].

For the case of the double scroll attractor, a candidate T for a trapping region has been presented in [15]. The set $T = \bigcup_{k=1}^{4} T_k$, is a union of the polygons T_k. The polygons T_1 and T_2 shown in Fig. 4 are subsets of the plane Σ_1, and enclose numerically observed sets R_1 and R_2. The sets $T_3, T_4 \subset \Sigma_2$ are symmetric to T_1 and T_2. The polygons T_1 and T_2 were constructed in such a way that for test points v_k belonging to their borders the conditions $P(v_k) \in T$ are verified in non-rigorous computations.

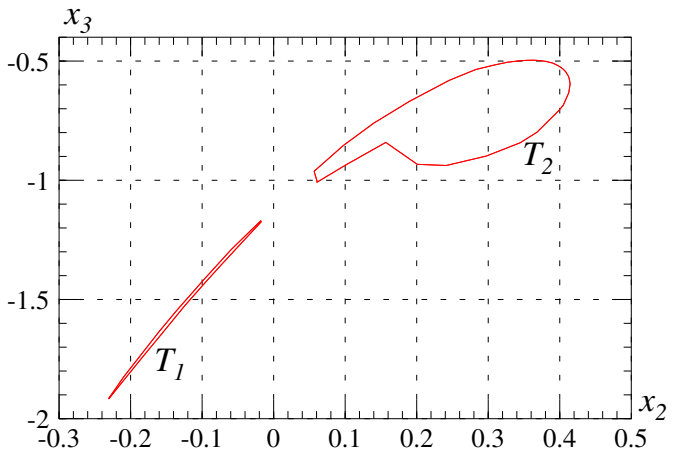

Fig. 4. Borders of polygons T_1 and T_2 defining the trapping region.

In this case, the method described above fails to prove that T is a trapping region. This happens because for a box $\mathbf{v}_k$

containing points which are mapped to T_2 and also containing points which are mapped to T_4 it is impossible to evaluate the return map P due to the discontinuity of P over $\mathbf{v}_k$. The discontinuity is a consequence of the fact that the double scroll attractor contains the origin—an unstable equilibrium. There are trajectories starting in T_1 which pass arbitrarily close to the origin. These trajectories are repelled from the origin along one of the two directions of its one-dimensional unstable manifold and reach either T_2 or T_4. Points in T_1 which are mapped to T_2 are separated from the points in T_1 which are mapped to T_4 by a curve belonging to the stable manifold of the origin. This curve separates points in R_1 plotted using different colors (compare Fig. 3). Trajectories initiated at the stable manifold converge to the origin and never come back to the set Σ. It follows that the return map is not even defined over the whole set T_1.

A rigorous evaluation of the return map for boxes containing discontinuity points requires to handle trajectories passing arbitrarily close to an equilibrium with infinitely large return times. This is relatively easy for linear systems for which the stable manifold is flat and explicit formulas for solution can be used. This approach was used for the Chua's circuit with a piecewise linear nonlinearity to prove the existence of a trapping region for the double scroll attractor [11]. For general nonlinear systems the stable manifold is not flat and a different approach has to be used (compare also [21]).

A. *Computation of trajectories passing close to an equilibrium*

In this section, we present a method how to compute trajectories of (1) in a neighborhood of the origin. The Jacobian matrix at the fixed point $x = (x_1, x_2, x_3)$ is

$$J(x) = \begin{pmatrix} -(R^{-1} + g_1 + 3g_2x_1^2)C_1^{-1} & R^{-1}C_1^{-1} & 0 \\ R^{-1}C_2^{-1} & -R^{-1}C_2^{-1} & C_2^{-1} \\ 0 & -L^{-1} & -R_0L^{-1} \end{pmatrix}. \quad (2)$$

For the equilibrium $\bar{x} = (0, 0, 0)$, we obtain

$$J \approx \begin{pmatrix} 0.128571429 & 0.714285714 & 0 \\ 0.064102564 & -0.064102564 & 0.128205128 \\ 0 & -0.528820730 & -0.007927023 \end{pmatrix}. \quad (3)$$

The matrix J has one real eigenvalue $\lambda \approx 0.2066098948$ and a pair of complex eigenvalues $\alpha \pm \beta i \approx -0.0750340265 \pm 0.1965518222i$. Let B be a transformation matrix converting the linear system $\dot{x} = Jx$ to the linear system $\dot{y} = Dy$ with the matrix D in the Jordan normal form

$$D = B^{-1}JB = \begin{pmatrix} \lambda & 0 & 0 \\ 0 & \alpha & \beta \\ 0 & -\beta & \alpha \end{pmatrix}. \quad (4)$$

We use the transformation matrix

$$B \approx \begin{pmatrix} -0.96026919 & 0.67812191 & 0 \\ -0.10491311 & -0.19329705 & 0.18660054 \\ 0.25860457 & -0.60865747 & -0.31225509 \end{pmatrix}. \quad (5)$$

The explicit solution of the linear dynamical system $\dot{y} = Dy$ with the initial condition $y(0) = (y_1(0), y_2(0), y_3(0))$ has the form $y_1(t) = e^{\lambda t}y_1(0)$, $y_2(t) = e^{\alpha t}(\cos(\beta t)y_2(0) + \sin(\beta t)y_3(0))$, $y_3(t) = e^{\alpha t}(-\sin(\beta t)y_2(0) + \cos(\beta t)y_3(0))$. The solution of the linear dynamical system $\dot{x} = Jx$ with the initial condition $x(0)$ can be computed as $x(t) = By(t)$, where $y(0) = B^{-1}x(0)$.

For the computer assisted proof enclosures of the matrix J, its eigenvalues, the transformation matrix B and its inverse are computed rigorously using interval arithmetic methods. For example, bounds for the eigenvalues are following: $\lambda \in 0.206609894821\,57^{55}_{49}$, $\alpha \in -0.075034026546\,00^{14}_{09}$, $\beta \in 0.196551822173727^{86}_{65}$, where subscripts and superscripts denote interval endpoints.

To handle trajectories passing close to the origin let us construct a cylinder centered at the origin spanned by the eigenvectors of J. Let us denote by $C_y(h, r) = \{y\colon |y_1| \le h, y_2^2 + y_3^2 \le r^2\}$ the cylinder centered at the origin with the height $2h > 0$ and the radius $r > 0$. Let $C_x(h, r) = BC_y(h, r)$ denote the cylinder $C_y(h, r)$ transformed by the change of coordinates $x = By$. The axis of $C_x(h, r)$ is the unstable one-dimensional eigenspace of the origin and bases of $C_x(h, r)$ are parallel to the stable eigenspace of the origin. The cylinder $C_x(h, r)$ with the height $2h = 0.008$ and the radius $r = 0.004$ is plotted in Fig. 5 in red. Four example trajectories passing through the cylinder are plotted in green and magenta. All four trajectories enter the cylinder through its side very close to the stable manifold of the fixed point at the origin and leave the cylinder through one of its bases near the unstable manifold.

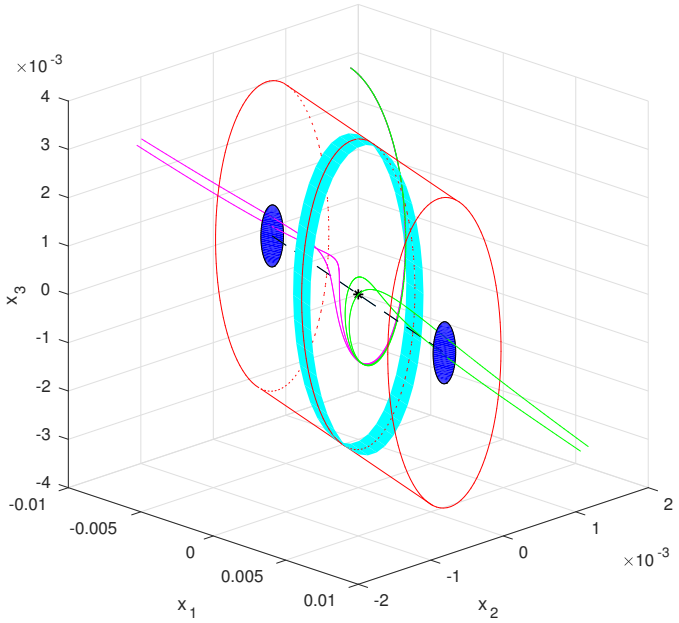

Fig. 5. Dynamics of the nonlinear system near the origin.

To compute enclosures of trajectories passing through the cylinder $C_x(h, r)$ we first find an enclosure $\mathbf{x}$ of the entry set, which contains intersections of trajectories with the cylinder's side and convert the enclosure $\mathbf{x}$ to the y coordinates via the transformation $y = B^{-1}x$. Then we modify the transformed entry set $\mathbf{y}$ to take into account perturbations introduced by the nonlinear change of coordinates to be applied for the computation of trajectories inside the cylinder. This is achieved

by inflating the interval vector $\mathbf{y}$ by a specific radius. The nonlinear change of coordinates is constructed in such a way that the nonlinear vector field (1) is transformed into an *almost linear* vector field $\dot{y} \approx Dy$ inside the cylinder. Next, we integrate the linear flow $\dot{y} = Dy$ inside the cylinder where the matrix D contains perturbed (set-valued) eigenvalues and find the exit set which is the intersection of trajectories initiated in the entry set with cylinder bases. In case the perturbed entry set has non-empty intersection with the stable eigenspace, the exit set is composed of two components, each enclosed in one of the cylinder's bases. Otherwise, the exit set is enclosed in a single cylinder's base. Finally, we modify the exit set to take into account perturbations introduced by the nonlinear change of coordinates, convert the exit set to the original coordinates using the transformation $x = By$ and continue integration using standard rigorous integration methods.

The main difficulty of the procedure is the construction of a nonlinear change of coordinates such that the nonlinear vector field (1) is transformed into something close to the linear vector field $\dot{y} = Dy$ inside the cylinder. In the construction the theory of normal forms is used. In general, the method is similar to the one used in [21] for the rigorous computation of trajectories passing close to the unstable equilibrium in the Lorenz attractor. The differences include stability types of the equilibrium and nonlinearities. For the Lorenz system the Jacobian matrix at the equilibrium has three real eigenvalues, while in our case there is one real eigenvalue and two complex ones. Regarding nonlinearities, for the Lorenz system the nonlinearity is of quadratic type, while here we have a cubic nonlinearity. Details of the construction procedure are skipped for the sake of brevity and will be reported elsewhere.

As mentioned before, the nonlinear change of coordinates introduces perturbations which have to be taken into account when computing cylinder's entry and exit points. For the cylinder $C_y(h, r)$ with the height $2h = 0.008$ and the radius $r = 0.004$ the bound for the entry perturbation is 3.303×10^{-6} and the bound for the exit perturbation is 3.307×10^{-6}. Additionally one has to take into account the perturbation of the eigenvalues which is bounded by 2.503×10^{-33}. This perturbation can be easily handled by inflating the entries of the matrix D into an interval matrix $\mathbf{D}$.

B. The existence of a trapping region for the double scroll attractor

The main result is stated in the following theorem.

Theorem 1: There exists a set $T \subset \Sigma$ enclosing the numerically observed double scroll attractor such that for each $x \in T$ either $P(x) \in T$ or the trajectory $\varphi(t, x)$ with the initial point x converges to the origin without intersecting Σ, i.e., $\varphi(t, x) \to (0, 0, 0)$ for $t \to \infty$ and $\{\varphi(t, x) \colon t > 0\} \cap T = \emptyset$.

The proof is carried out for the set $T = \bigcup_{k=1}^{4} T_k$ defined previously (see Fig. 4). From the symmetry of the problem it is sufficient to verify the conditions stated in the theorem for the set $T_1 \cup T_2$. First, we prove that $P(T_2) \subset T_1$. This is done using a standard rigorous integration method in the same way as for the spiral attractor.

The proof regarding the set T_1 consists of three steps. In the first step, we prove that for each $x \in T_1$ either $P(x) \in T$ or the trajectory with the initial point x enters the cylinder $C_x(\bar{h}, r)$ through its side, where $\bar{h} < h$. By selecting $\bar{h}$, we control the distance between a cylinder entry point and the stable eigenspace. The entry set satisfying the condition $|(B^{-1}x)_1| = |y_1| \leq \bar{h}$ for $\bar{h} = 2\times10^{-4}$ is plotted in Fig. 5 in cyan. We use the method of generalized bisection. The list of boxes to be processed is created by covering T_1 by boxes $\mathbf{v}_k$ of a fixed size. For each box $\mathbf{v}_k$, we attempt to find an enclosure of $P(\mathbf{v}_k)$. If the procedure succeeds and the image is enclosed in T then we remove the box $\mathbf{v}_k$ from the list. In the opposite case, we try to evaluate the return map P_C with the section being the side of the cylinder $\{(x_1, x_2, x_3) \colon y_2^2 + y_3^2 = r^2, \text{ where } y = B^{-1}x\}$. If these computations are successful and the distance between the entry set and the stable eigenspace is smaller than $\bar{h}$ (the condition $|y_1| = |(B^{-1}x)_1| \leq \bar{h}$ is used) then we remove this box from the list of boxes. If none of these two procedures are successful then the box $\mathbf{v}_k$ is split into smaller boxes which are added to the list of boxes to be processed. The computations are continued until the list of boxes is empty. Computations in this step have been completed for $\bar{h} = 5 \times 10^{-5}$.

In the second step, we show that all trajectories initiated inside the cylinder $C_x(\bar{h}, r)$ either converge to the origin or exit through one of the sides of the cylinder $C_x(h, \bar{r})$ with the radius $\bar{r} = 0.00084$. In these computations the entry and exit perturbation has been taken into account. The exit sets with radius $\bar{r}$ are plotted in blue in Fig. 5.

In the third step of the procedure, we prove that all trajectories with initial points belonging to exit sets return to T_2 or T_4. This is done by covering the exit sets by boxes $\mathbf{v}_k$, evaluating the return map on these boxes and verifying that one of the inclusions $P(\mathbf{v}_k) \subset T_2$ or $P(\mathbf{v}_k) \subset T_4$ holds. This completes the computer assisted proof of Theorem 1.

Details regarding the computer-assisted proof are following. The border of T_2 is covered by 1187 boxes and it is shown that their images are enclosed in T_1. The border of T_1 is covered by 5133 boxes. For 5101 boxes it was proved using standard rigorous integration methods that their images are enclosed in $T_1 \cup T_2$. For the remaining 32 boxes it was shown that the corresponding trajectories enter the cylinder $C_x(\bar{h}, r)$.

In [15], it was shown that the return map P restricted to the trapping region T has positive topological entropy. It follows that the set T contains infinitely many periodic orbits and chaotic trajectories.

IV. Conclusions

A method to find enclosures of trajectories passing arbitrarily close to an unstable equilibrium has been presented. Using this method the existence of a trapping region for the double scroll attractor observed for the Chua's circuit with a cubic nonlinearity has been proved.

Acknowledgment

This work was supported in part by the AGH University of Science and Technology, grant no. 11.11.120.343.

References

[1] L. O. Chua, M. Komuro, and T. Matsumoto, "The double scroll family," *IEEE Trans. Circuits Syst.*, vol. 33, pp. 1037–1118, Nov. 1986.

[2] F. Ayrom, , and G. Zhong, "Chaos in Chua's circuit," *IEE Proceedings D - Control Theory and Applications*, vol. 133, no. 6, pp. 307–312, 1986.

[3] T. Matsumoto, L. O. Chua, and K. Ayaki, "Reality of chaos in the double scroll circuit: A computer-assisted proof," *IEEE Trans. Circuits Syst.*, vol. 35, no. 7, pp. 909–925, July 1988.

[4] L. O. Chua, "Global unfolding of Chua's circuit," *IEICE Trans. Fundam.*, vol. 76, no. 5, pp. 704–734, 1993.

[5] M. Komuro, R. Tokunaga, T. Matsumoto, L. O. Chua, and A. Hotta, "Global bifurcation analysis of the double scroll circuit," *Int. J. Bifurcation Chaos*, vol. 1, no. 1, pp. 139–182, 1991.

[6] R. N. Madan, *Chua's Circuit: A Paradigm for Chaos*. Singapore: World Scientific, 1993.

[7] Z. Galias, "Positive topological entropy of Chua's circuit: A computer assisted proof," *Int. J. Bifurcation Chaos*, vol. 7, no. 2, pp. 331–349, 1997.

[8] S. Boughaba and R. Lozi, "Fitting trapping regions for Chua's attractor — a novel method based on isochronic lines," *Int. J. Bifurcation Chaos*, vol. 10, no. 1, pp. 205–225, 2000.

[9] Y. Yang, Z. Duan, and L. Huang, "Robust dichotomy analysis and synthesis with application to an extended Chua's circuit," *IEEE Trans. Circuits Syst. I*, vol. 54, no. 9, pp. 2078–2086, 2007.

[10] B. Bao, P. Jiang, Q. Xu, and M. Chen, "Hidden attractors in a practical Chua's circuit based on a modified Chua's diode," *Electronics Letters*, vol. 52, no. 1, pp. 23–25, 2016.

[11] Z. Galias, "Trapping region for the double scroll attractor," in *Proc. IEEE Int. Symp. Circuits Syst. (ISCAS)*, May 2012, pp. 401–404.

[12] ——, "Rigorous study of the Chua's circuit spiral attractor," *IEEE Trans. Circuits Syst. I*, vol. 59, no. 10, pp. 2374–2382, 2012.

[13] A. Khibnik, D. Roose, and L. O. Chua, "On periodic and homoclinic bifurcations in Chua's circuits with a smooth nonlinearity," *Int. J. Bifurcation Chaos*, vol. 3, no. 2, pp. 363–384, 1993.

[14] G. Zhong, "Implementation of Chua's circuit with a cubic nonlinearity," *IEEE Trans. Circuits Syst. I*, vol. 41, no. 12, pp. 934–941, 1994.

[15] Z. Galias, "Rigorous analysis of Chua's circuit with a smooth nonlinearity," *IEEE Trans. Circuits Syst. I*, vol. 63, no. 12, pp. 2304–2312, Dec 2016.

[16] G. Leonov, N. Kuznetsov, and V. Vagaitsev, "Hidden attractor in smooth Chua systems," *Physica D: Nonlinear Phenomena*, vol. 241, no. 18, pp. 1482–1486, 2012.

[17] Z. Galias, "The dangers of rounding errors for simulations and analysis of nonlinear circuits and systems — and how to avoid them," *IEEE Circuits Syst. Mag.*, vol. 13, no. 3, pp. 35–52, 2013.

[18] R. J. Lohner, "Computation of guaranteed enclosures for the solutions of ordinary initial and boundary value problems," in *Computational Ordinary Differential Equations*, J. Cash and I. Gladwell, Eds. Oxford: Clarendon Press, 1992.

[19] O. Knüppel, "PROFIL/BIAS—a fast interval library," *Computing*, vol. 53, no. 3–4, pp. 277–287, 1994.

[20] "CAPD library," http://capd.ii.uj.edu.pl/, 2016.

[21] W. Tucker, "The Lorenz attractor exists," *C. R. Acad. Sci. Paris*, vol. 328, pp. 1197–1202, 1999.